

Article

A Knowledge-Guided Intelligent Analysis Method of Geographic Digital Twin Models: A Case Study on the Diagnosis of Geometric Deformation in Tunnel Excavation Profiles

Ce Liang, Jun Zhu *, Jinbin Zhang, Qing Zhu, Jingyi Lu, Jianbo Lai and Jianlin Wu

Faculty of Geosciences and Environmental Engineering, Southwest Jiaotong University, Chengdu 610031, China; qinchii@my.swjtu.edu.cn (C.L.); zhangjinbin@my.swjtu.edu.cn (J.Z.); zhuqing@swjtu.edu.cn (Q.Z.); ljiy08@my.swjtu.edu.cn (J.L.); ljb2244@my.swjtu.edu.cn (J.L.); wujianlin@my.swjtu.edu.cn (J.W.)

* Correspondence: zhujun@swjtu.edu.cn

Abstract: It is essential to establish a digital twin scene, which helps to depict the dynamically changing geographical environment accurately. Digital twins could improve the refined management level of intelligent tunnel construction; however, research on geographical twin models primarily focuses on modeling and visual description, which has low analysis efficiency. This paper proposes a knowledge-guided intelligent analysis method for the geometric deformation of tunnel excavation profile twins. Firstly, a dynamic data-driven knowledge graph of tunnel excavation twin scenes was constructed to describe tunnel excavation profile twin scenes accurately. Secondly, an intelligent diagnosis algorithm for geometric deformation of tunnel excavation contour twins was designed by knowledge guidance. Thirdly, multiple visual variables were jointly used to support scene fusion visualization of tunnel excavation profile twin scenes. Finally, a case was selected to implement the experimental analysis. The experimental results demonstrate that the method in this article can achieve an accurate description of objects and their relationships in tunnel excavation twin scenes, which supports rapid geometric deformation analysis of the tunnel excavation profile twin. The speed of geometric deformation diagnosis is increased by more than 90% and the cognitive efficiency is improved by 70%. The complexity and difficulty of the deformation analysis operation are reduced, and the diagnostic analysis ability and standardization of the geographic digital twin model are effectively improved.

Keywords: geographic digital twins; knowledge graph; tunnel excavation profile; geometric deformation diagnosis; fusion visualization



Citation: Liang, C.; Zhu, J.; Zhang, J.; Zhu, Q.; Lu, J.; Lai, J.; Wu, J. A Knowledge-Guided Intelligent Analysis Method of Geographic Digital Twin Models: A Case Study on the Diagnosis of Geometric Deformation in Tunnel Excavation Profiles. *ISPRS Int. J. Geo-Inf.* **2024**, *13*, 78. <https://doi.org/10.3390/ijgi13030078>

Academic Editors: Wolfgang Kainz and Songnian Li

Received: 17 December 2023

Revised: 17 February 2024

Accepted: 28 February 2024

Published: 29 February 2024



Copyright: © 2024 by the authors. Licensee MDPI, Basel, Switzerland. This article is an open access article distributed under the terms and conditions of the Creative Commons Attribution (CC BY) license (<https://creativecommons.org/licenses/by/4.0/>).

1. Introduction

The geographical environment is a highly complex dynamic system where multiple factors such as climate, topography, hydrology, soil, and biology interact and influence each other, resulting in continuous and uncertain dynamic changes. Such changes pose significant challenges for the future development of human society [1–3]. Tunnel excavation projects are typical examples influenced by changes in the geographical environment. Environmental factors, such as geotechnical mechanics, could change the tunnel excavation profile, resulting in construction safety and project quality problems [4,5].

In recent years, with the development of geographical digital twin technologies, intelligent construction has gradually become an essential direction for tunnel excavation [6,7]. By constructing a digital twin geographical scene of tunnel excavation and establishing a dynamic connection between the physical world and the information world, it is possible to accurately control changes in tunnel excavation, which can alleviate or even eliminate the problem of over- and under-excavation during the construction process [8,9]; however,

current geographical twin models in tunnel engineering primarily focus on modeling and visual description, and there are few studies in which digital twin ideas are integrated into deformation diagnosis during construction [10–12]. The lack of diagnostic analysis functions has become a significant obstacle to achieving intelligent construction and precise management of tunnel projects. It is necessary to use fast and automatic geometric deformation analysis methods to improve the diagnostic capabilities of tunnel excavation profile twins [13,14].

Currently, common methods for analyzing the geometric deformation of tunnel excavation profiles include traditional instrument measurements, finite element analysis, and 3D laser scanning. Traditional measuring instruments (total stations and profilers) provide precise measurements and monitoring of tunnel excavation profiles, which directly reflect the deformation and stability of structures. This type of method is the most widely used in practical engineering [15,16]; however, such methods tend to ignore local micro-deformations, the processing process is long, and labor costs are enormous, which is not suitable for the requirements of intelligent construction. The finite element analysis method obtains the response and behavior rules of the tunnel structure under different conditions through simulation and analysis based on considering the tunnel boundary parameters and geological rock properties [17,18]. This method analyzes the deformation mechanism of tunnel excavation but it requires a lot of time to re-establish the analysis model when the geological structure changes. It lacks real-time and accurate capabilities, making it unsuitable for the requirements of tunnel excavation digital twins. Three-dimensional laser scanning technology could rapidly and accurately obtain the three-dimensional shape and surface features of the tunnel structure with millimeter-level accuracy. This type of method is very suitable for the construction of tunnel excavation profile twins, which provides adequate data support for comprehensive monitoring and rapid diagnosis of large-scale structures [19–22].

However, the tunnel construction environment is complex and changeable. Tunnel excavation is a continuously dynamic process with many influencing factors and complex relationships [23]. Existing diagnostic methods are difficult to directly apply to tunnel excavation profile twins, leading to problems such as difficulty in identifying dynamic deformation, low diagnostic efficiency, and low intelligence [24]. In addition, existing tunnel excavation profile twins lack appropriate semantic constraints and domain knowledge guidance in visual expression, resulting in difficulty and irregularity in user analysis and the user's cognitive efficiency needs to be improved.

In response to the above problem, this paper innovatively introduces knowledge graph technology into the tunnel excavation process based on the existing achievements of digital twins in tunnel construction. A knowledge-guided intelligent analysis method for the geometric deformation of tunnel excavation profile twins is proposed in this paper. Firstly, considering the dynamic changes in the tunnel excavation process, a dynamic data-driven knowledge graph of the tunnel excavation twin scene was established. Secondly, a knowledge-guided intelligent diagnosis algorithm for geometric deformation of tunnel excavation profile twins was proposed to improve the efficiency and accuracy of geometric deformation diagnosis. Finally, a fusion visualization method of tunnel excavation twin scenes driven jointly by multiple visual variables was developed, which reduces the complexity and difficulty of analysis and improves the degree of standardization.

2. Methods

2.1. Framework

Figure 1 illustrates the overall framework of this paper, which consists mainly of four parts: the construction of the tunnel excavation profile scene knowledge graph, geometric deformation diagnosis of the tunnel excavation profile, fusion visualization of the tunnel excavation twin scene, and case experiment analysis. Firstly, we establish a domain ontology model and dynamically extract knowledge based on multi-source data of tunnel construction scenarios to construct a 3D visual knowledge graph of the tunnel excavation

profile twin. Secondly, we establish a knowledge graph-guided geometric deformation diagnosis of the tunnel excavation profile algorithm to analyze the deformation over-limit behavior of tunnel excavation. At the same time, based on the tunnel structure information and deformation diagnosis results, we combine multiple visual variables to achieve the fusion expression of the tunnel excavation diagnostic information. Finally, we conduct a case experiment analysis to ensure the effectiveness and feasibility of this method.

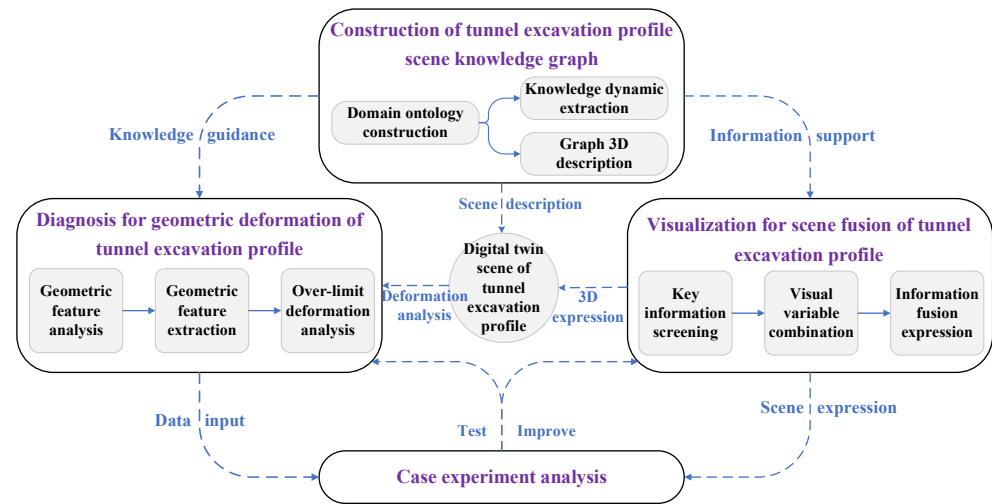


Figure 1. Overall framework.

2.2. Dynamic Data-Driven Construction of Knowledge Graphs for Twin Tunnel Excavation Scene

Tunnel excavation is a dynamic process that evolves over time. As time goes by, information on the tunnel excavation process—such as the surrounding rock level, mileage information, and tunnel structure—is constantly and iteratively updated. Utilizing these data to dynamically construct a knowledge graph cannot only accurately describe the tunnel excavation process but also accumulate knowledge for future excavation work [25–28]. The construction process of the knowledge graph is illustrated in Figure 2.

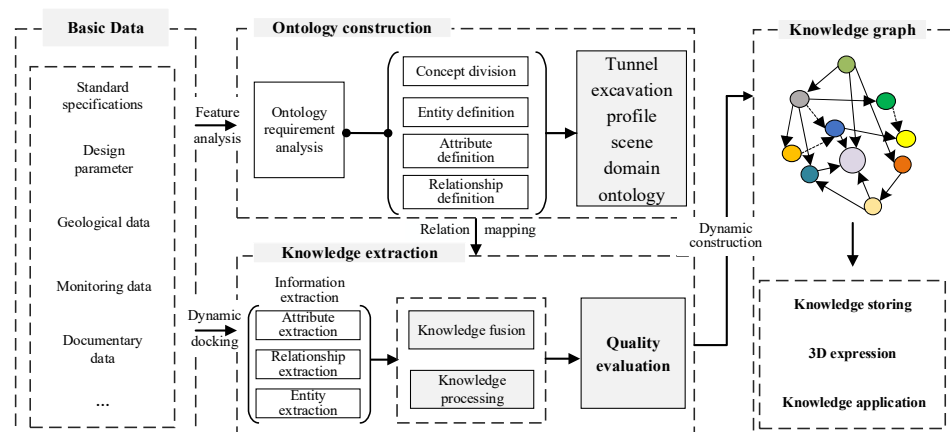


Figure 2. Knowledge graph construction method of tunnel excavation twin scene.

Firstly, feature analysis is performed on basic data of the tunnel excavation, such as standard specifications, design parameters, geographic data, and monitoring data. These data are categorized into static features that do not change during the excavation process and dynamic data that continually change with the excavation progress. After that, based on the results of data analysis, knowledge modeling for the tunnel excavation takes place. This involves dividing concepts, defining entities, establishing a domain ontology of the

tunnel excavation profile scene for the content, and forming the establishment of knowledge expression. Furthermore, according to the structure of the ontology, the corresponding entities, attributes, and relationships are extracted from the dynamic data. The extracted content is then integrated, processed, and quality assessed to ensure the integrity and validity of the knowledge. Finally, based on the extracted knowledge, the knowledge graph is constructed, stored, and 3D expressed. This knowledge graph is then applied to the integral and dynamic construction of the knowledge graph, resulting in its realization.

As far as domain ontology is concerned, it aims to provide a shared, standardized, precise, and reusable conceptual framework. Knowledge interaction and information sharing between different systems require the induction, abstraction, and modeling of the conceptual system in the field. To achieve tunnel field modeling in this paper, firstly, based on the long-line construction characteristics of the tunnel, the tunnel ontology model entities are divided into tunnel structure entities (such as tunnel lining, guide tunnels, inverts, etc.), construction section entities (mileage start, mileage length, etc.), contour features (curves, etc.), radius (center point coordinates, etc.), construction environment (surrounding rock grade, groundwater level, etc.), construction information (construction equipment, support library, etc.). Secondly, the entity relationships and attributes in the ontology are predefined. The entity relationship describes the interconnection status between entities, which is equivalent to the bridge between things; the entity attributes describe the detailed information inside the entity and increase the user's understanding of the essence of things, mainly including the hypernym relationship (taking the ontology relationship of the tunnel structure as an example, the inverted arch can be regarded as the hypernym of lining, and the lining is the hypernym of the guide tunnel), semantic association relationships (tunnel design geometric parameters, material property characteristics, etc.), and spatio-temporal coupling relationships (construction mileage connection relationships, spatial relationships, etc.). Based on the content mentioned above, a clear conceptual hierarchical structure relationship is formed, and the tunnel ontology model is shown in Figure 3.

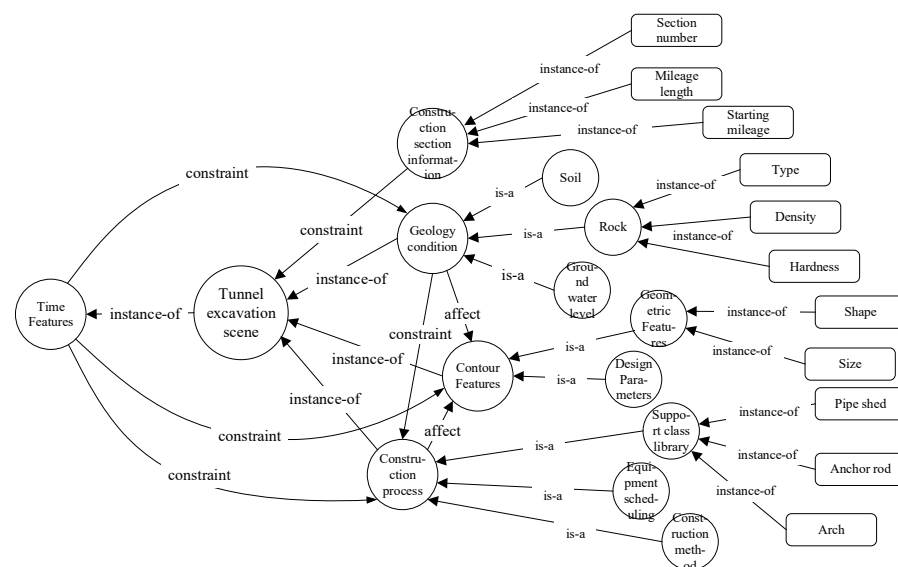


Figure 3. Tunnel excavation twin scene ontology model.

2.3. Knowledge-Guided Geometric Deformation Intelligent Diagnosis Algorithm of Tunnel Excavation Profile Twin

It is necessary to diagnose the deformation of the contour structure in the process of tunnel excavation to prevent excessive deformation from affecting the safety of the construction project. The amount of over-under-excavated tunnel is uncontrollable, and the deformation monitoring points and deformation variables will also change. In order to solve the problems with low accuracy and incomplete analysis of tunnel deformation

detection, this paper innovatively introduces the knowledge graph. A knowledge-guided intelligent diagnosis algorithm for the geometric deformation of a twin in-tunnel excavation profile was proposed to improve the efficiency and accuracy of geometric deformation diagnosis. Firstly, based on the twin scene knowledge graph of the tunnel excavation, the geometric features of the tunnel excavation profile are constrained in knowledge guidance to determine the search threshold of the deformation range, which provides a basis for deformation over-limit analysis. Secondly, the line-surface feature constraints of the geometric extraction algorithm for the deformation information of tunnel excavation twin are established, which achieves the accurate extraction of tunnel contour deformation geometric features. Finally, through knowledge guidance, the intelligent diagnosis algorithm of tunnel geometric deformation is designed. The efficient diagnosis and analysis for geometric deformation of the tunnel excavation profile twin is achieved, which is used to update and iterate the tunnel twin, as shown in Figure 4.

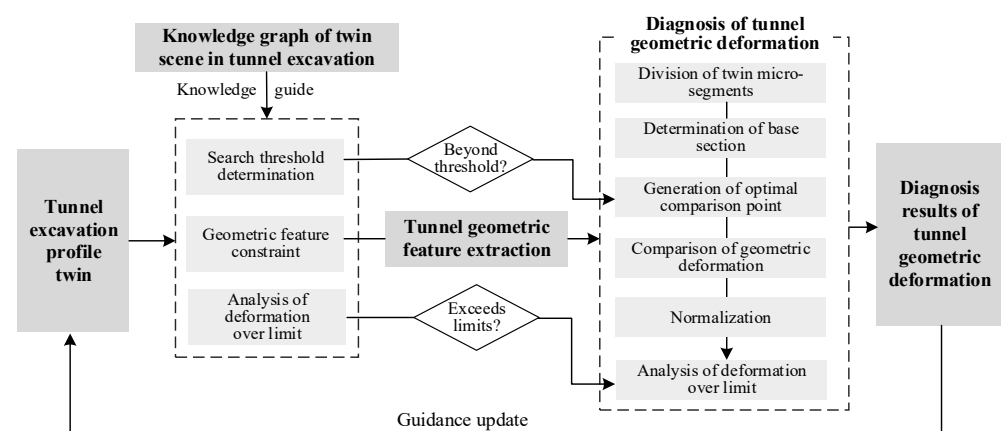


Figure 4. Intelligent diagnosis algorithm of twin geometric deformation.

First, based on the knowledge graph, an algorithm is designed to calculate the deformation search threshold of the tunnel excavation scene. Based on the spatial position correlation calculation, the spatial correlation strength between the deformation monitoring position of the tunnel excavation scene and the tunnel scene structure is determined. A knowledge correlation network is established to support the space search threshold S calculation for geometric deformation of the tunnel excavation. According to the spatial semantic correlation S_s , spatial proximity S_p , and spatial overlap S_o , the search threshold calculation formula is shown in Formula (1):

$$S = \omega_s \times S_s + \omega_p \times S_p + \omega_o \times S_o \quad (1)$$

where ω_s , ω_p , and ω_o are the weight factors corresponding to each parameter. The sum of the weight factors is 1, and their settings are related to the actual geometric deformation degree of the tunnel at different construction stages.

Next, we establish an algorithm for geometric deformation information extraction of the tunnel excavation twins constrained with line-surface feature constraints. Accurate extraction of tunnel excavation contours is the key to geometric deformation analysis. Taking the direction of the central axis of the tunnel as the benchmark to determine the direction of micro-segment division and record it as $\vec{m} = (A, B, C)$. For each division unit, due to the limited number of point clouds that intersect with the normal plane, the point set obtained by direct intersection may be sparse and difficult to summarize the real profile information, further affecting the centroid solution. Therefore, it is necessary to expand the point cloud quantity where the normal plane is located. Using the normal plane as the reference, and slicing it after extending the distance d forward and backward to make a slice, all the inner points of the slice orthogonally project to the normal plane. The true

coordinates of any projected point P_{op} can be calculated using Formula (2), from which the tunnel excavation profile can be obtained.

$$\begin{cases} x_{op} = \frac{(B^2+C^2)x_m - A(By_m+Cz_m+D_i)}{A^2+B^2+C^2} \\ y_{op} = \frac{(A^2+C^2)y_m - B(Ax_m+Cz_m+D_i)}{A^2+B^2+C^2} \\ z_{op} = \frac{(A^2+B^2)z_m - C(Ax_m+By_m+D_i)}{A^2+B^2+C^2} \end{cases} \quad (2)$$

where $P_m(x_m, y_m, z_m)$ is any point in the slice of N_i ; $P_{op}(x_{op}, y_{op}, z_{op})$ is the coordinate of the projection point on the normal plane of the point in the slice.

After the geometric feature extraction of the tunnel excavation profile is completed, the over-under-excavation results of the tunnel excavation profile can be quickly analyzed based on the comparison of the theoretical model with the measurement model. By comparing the two-phase measurement models, the geometric deformation of the tunnel excavation profile can be diagnosed. Since there are some uncontrollable implicit data operations in the methods of calculating point clouds to the best-fitting plane and mesh surfaces, this paper chooses to calculate deformations by directly comparing the distances between individual points within the point cloud. Calculating the Euclidean distance d from each point p in the point cloud P to the nearest neighbor point in the reference point cloud R as the local distance. As shown in Formula (3), the cloud-to-cloud distance problem is converted into a point-to-point distance calculation.

$$d(p, R) = \min_{r \in R} \|p - r\|_2 \quad (r < S) \quad (3)$$

where S is the deformation search threshold.

This is an approximate estimation method, which does not consider the point cloud surface and only searches for points but is fast and straightforward; however, this method requires calculating the distance from the point to all points within the neighbor points. The setting of the neighbor points' size and the density of the reference point cloud will affect the calculation speed. This paper optimizes the corresponding point search results through the interpolation method. For the reference point cloud, an interpolation grid is established in a plane orthogonal to the point cloud deformation direction. The corresponding points on the grid orthogonal to the comparative point cloud are established. Gaussian regression is performed on the data grid point where each corresponding point is located. Estimating the true position of actual point pairs through this method achieves a higher-precision deviation calculation, which further provides a more comprehensive twin geometric deformation evaluation of the tunnel excavation profile twin using multiple evaluation parameters. The schematic diagram of the intelligent diagnosis of the twin geometric deformation is shown in Figure 5.

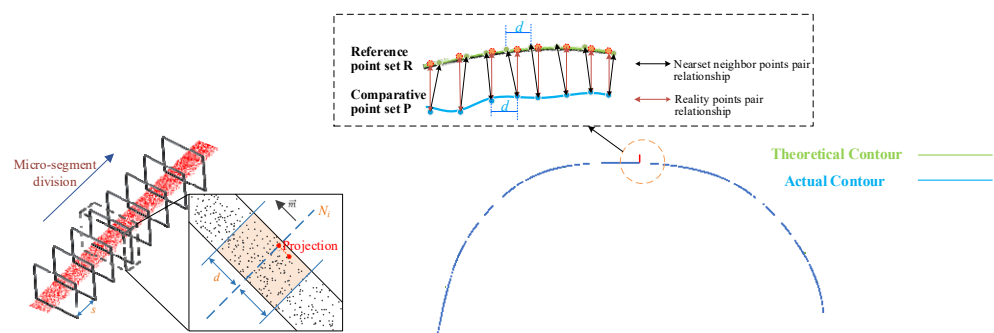


Figure 5. Schematic diagram for intelligent diagnosis of geometric deformation twin.

In order to ensure the accuracy of the deformation intelligent diagnosis results and the correct use of later construction guidance, the accuracy of the results is evaluated

before use. P_R and P_V , respectively, represent the reference point cloud and the result to be evaluated. When calculating the error between the two, P_R and P_V are used as references, respectively, to calculate the Euclidean geometric distances $D_{R,V}$ and $D_{V,R}$ between the two points, as shown in Figure 6.

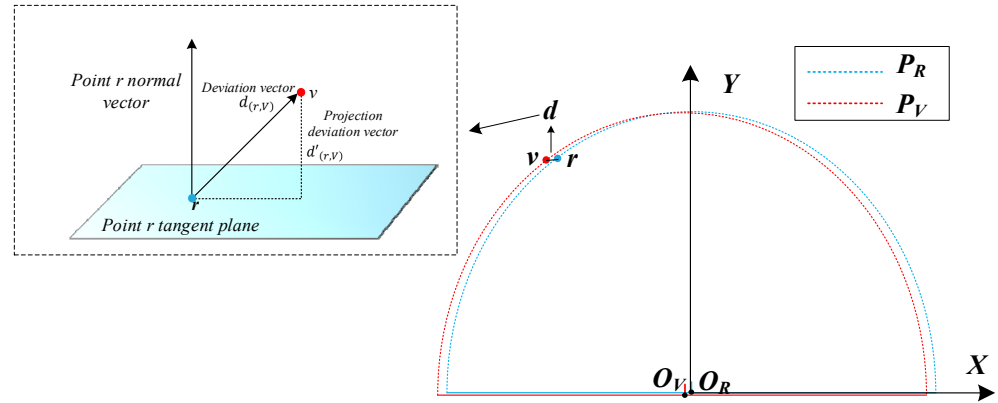


Figure 6. Tunnel deformation diagnostic accuracy assessment.

For each point r in P_R , the corresponding point v in P_V is found using the nearest neighbor method. If the point cloud normal vector of point r is N_r , then the distance calculations for point r and point cloud P_V based on point-to-point and point-to-plane are as follows:

$$d_{P2P}(r, P_V) = \|\vec{d}_{r,P_V}\|_2^2 \quad (4)$$

$$d_{P2L}(r, P_V) = \left(\vec{E}_{r,P_V} \cdot N_r \right)^2 \quad (5)$$

Due to the non-corresponding characteristics of point clouds, the point errors between the reference point cloud and the point cloud to be evaluated are usually asymmetrical. The correct comparison result cannot be obtained, and the larger error value is taken as the accuracy evaluation result of P_v , which is the maximum value of the two errors ($\max(D(P_R, P_V), D(P_V, P_R))$) taken. Finally, in order to better quantify the error, the error values are standardized.

$$F = 10 \log_{10} \left(\frac{P_v^2}{\max(D(P_R, P_V), D(P_V, P_R))} \right) \quad (6)$$

2.4. Multivariate Visual Variable Integration in the Digital Twin Visualization of Tunnel Excavation Scenes

Visualization methods enhance human understanding of complex information by displaying data features in an intuitive and attractive way [29–33]. In order to improve users' accurate understanding of this key information when conveying diagnostic information about tunnel excavation deformation, this information must be transformed into easy-to-understand visual variables [34–38]. The digital twin scenes of tunnel excavation are complex and changeable. They not only contain information about the tunnel excavation section but also involve multi-dimensional data such as geotechnical properties, supporting structures, and construction equipment. These complex information elements may interfere with people's effective visual search, leading to an increase in cognitive load. Therefore, a visualization method of multi-visual variable fusion is proposed, as shown in Figure 7.

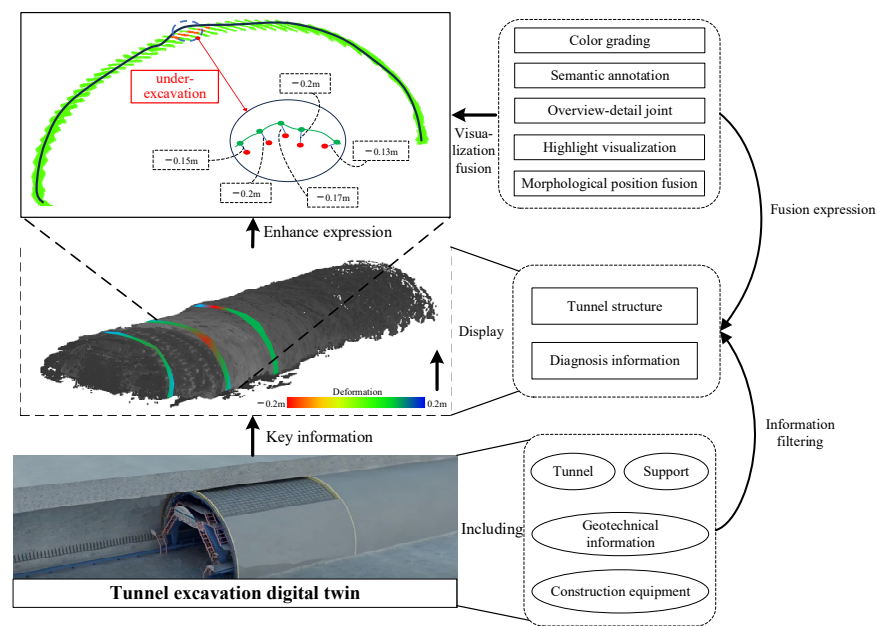


Figure 7. Tunnel excavation twin scene fusion visualization method.

Firstly, content screening is performed to prioritize the focus of the information, which includes the tunnel structure and excavation diagnostic information. Next, the tunnel structure is presented in the form of a 3D model to demonstrate its geometric properties. The diagnostic information uses a layered coloring method, integrating with the tunnel 3D model for display. The introduction of color bands helps users with visual positioning and search, enabling them to quickly and accurately obtain key diagnostic results. Furthermore, considering that minute deformations of centimeters or even millimeters may occur during tunnel excavation, enhanced expression is performed based on diagnostic information. This enhancement method displays the over–under-excavation status of the tunnel by zooming in on local details of the excavation location while using semantic annotations to assist in the interpretation of diagnostic information. Finally, integrating the above information expression methods to establish an overview–detail visualization method that combines multiple visual variables to improve users’ cognitive efficiency of complex tunnel excavation information.

3. Experiments and Results

3.1. Case Study

A case study was conducted on an extra-long tunnel for deformation diagnosis analysis of the tunnel excavation profile. The tunnel is a single-bore tunnel with a total length of 11.75 km and a maximum burial depth of approximately 550 m. It is a double-track tunnel within a single bore. The geological conditions of the tunnel are complex, crossing multiple rock contact zones along the alignment. The lithology is complex and changeable, with developed local joints and fissures, resulting in poor integrity of the rock mass. There are several sections of high-temperature environments and extremely high-stress sections, making it one of the critical control projects on the entire rail line. By collecting data on the tunnel scene multiple times during the construction process, a twin tunnel excavation scene was constructed (Figure 8).

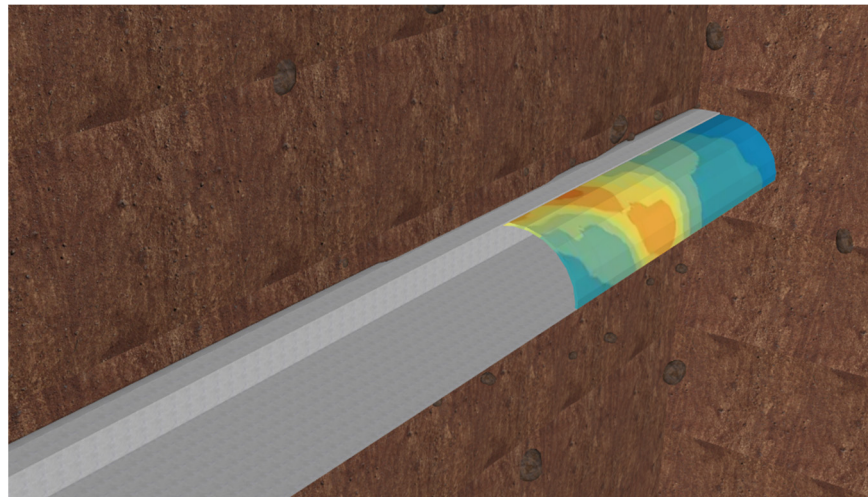


Figure 8. Tunnel excavation twin scene.

At the same time, a knowledge graph was constructed based on the multi-source data of tunnel excavation. A total of 36 entity nodes and 202 relationships were selected. A Neo4j graph database was used to store these nodes and relationships. Finally, a knowledge graph of the twin scenes of the tunnel excavation was formed to accurately depict the entities and relationships of the twin scenes (Figure 9).

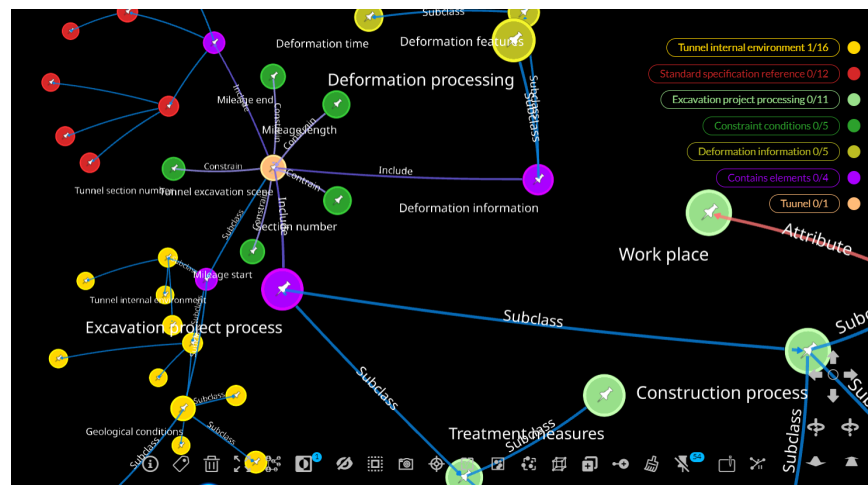


Figure 9. Knowledge graph of tunnel excavation twin scene.

We constrained the tunnel twin model through tunnel segment attribute information to distinguish the tunnel twin knowledge data of different segments. The excavation contour knowledge is dynamically extracted during the forward excavation process of the tunnel project, which can help the tunnel excavation scene knowledge storage and the excavation stage form a corresponding relationship, and the content of the knowledge graph is continuously updated. It guided the diagnosis and visualization process of complex tunnel excavation scenarios, reducing the difficulty and complexity of diagnosis and visualization.

The experiment takes the tunnel excavation section DK49+574 as an example, recording the section number and other attribute information and synchronously updating the knowledge of the twin scenario of this tunnel section in the knowledge base. When analysis is required for a specific feature point, the surrounding rock grade is determined through the knowledge base. Utilizing the knowledge data stored in the knowledge graph, combined with other environmental conditions and excavation environments affecting

the point, the type and degree of geometric deformation of the point are analyzed. It is determined that the point has undergone curvature deformation, and the deformation level is classified as first-level curvature deformation. The geometric diagnosis results can provide effective guidance for subsequent construction during the excavation process. The common construction treatment measures for first-level curvature deformation involve mild interventions, such as strengthening observation records and adjusting excavation speed, etc. (Figure 10).

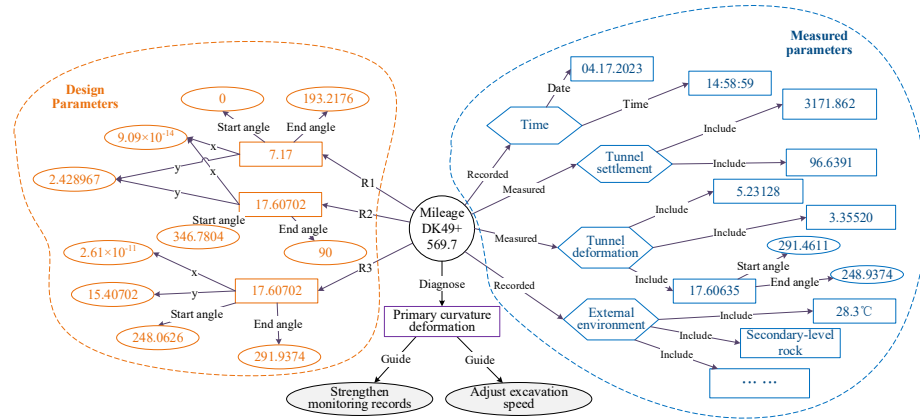


Figure 10. Excavation scene ontology model of tunnel DK49+574 section.

In the subsequent excavation process, the same method is used to dynamically update the twin scene knowledge of the newly excavated tunnel section. At the same time, the prior knowledge of the excavated section can guide the subsequent construction and update of the knowledge map, forming a knowledge-guided tunnel digital twin model geometric deformation diagnosis and visualization.

3.2. Experimental Results and Analysis

To test the intelligent analysis method of geometric deformation of tunnel excavation profile twins proposed in this article, the system server was built using Node.js v6.11.2. Neo4j community 4.4.2 was used to store graph data. The browser was built using HTML5, CSS3, and JavaScript. The 3D rendering engine digital twin platform was built through the open-source virtual earth Cesium.js v1.45. The program ran on Google Chrome 192.168.101.201.103. Based on the development environment mentioned above, the twin geometric feature extraction and deformation diagnosis of the tunnel excavation and the visual cognition experiments were carried out. The environment configuration information involved in these experiments is listed in Table 1.

Table 1. Development environment configuration.

	Content	Details
Hardware	CPU	Intel I(TM) i5-10210U CPU @1.60 GHz 2.11 GHz GIntel(R) UHD Graphics
	Memory Eye tracker	16 GB Tobii Pro Spectrum
Software	IDE	Visual Studio 2019
	System server	Node.js v6.11.2
	Graph database	Neo4j community 4.4.2
	Digital twin platform System	Cesium.js v1.45 Windows 10

3.2.1. Tunnel Geometric Deformation Diagnosis Experiment and Analysis

Based on the spatial geometric relationship in the knowledge graph, the geometric feature-constraint of the tunnel profile is performed. The geometric features of the tunnel are mainly the linear tunnel section. Based on the technical method proposed in Section 2.3 of this paper, the geometric features of the twin point cloud of tunnel excavation are extracted after preprocessing. Taking the excavation profile of DK49+575 tunnel as an example, the geometric feature extraction of tunnel excavation contour is carried out, and the tunnel excavation twin data are divided into micro-segments with a thickness of 1 cm and an interval of 10 cm, as illustrated in Figure 11a. After the reference section is determined, the actual excavation contour feature line is obtained by generating the optimal comparison point set of the tunnel excavation contour, as illustrated in Figure 11b.

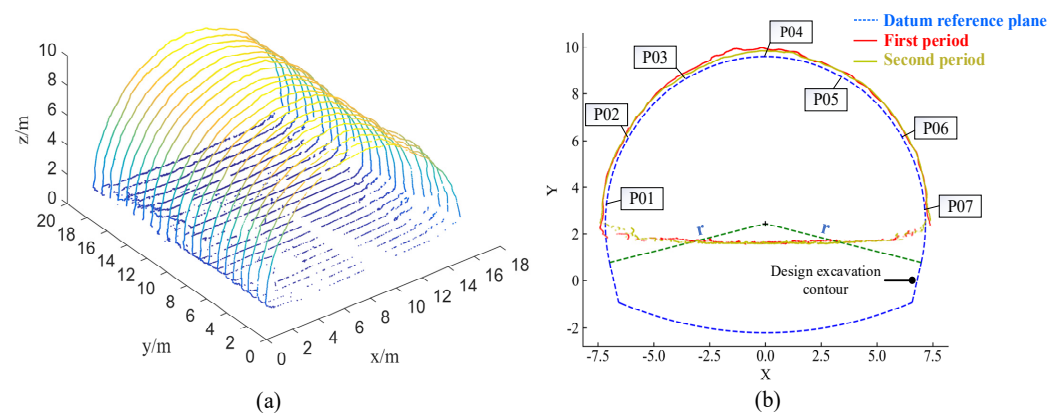


Figure 11. Tunnel point cloud slicing and cross-section analysis results. (a) Division of tunnel twin micro-segments. (b) Tunnel datum and actual excavation contour characteristic line.

Based on the tunnel data and the actual excavation contour feature line extraction results, deformation diagnosis and analysis were conducted. The results are illustrated in Table 2, and the deformation results in Figure 12. From the experimental results, monitoring points P01~P07 from the two phases of data are located on the periphery of the design curve, with monitoring points P04 and P05 being the furthest from the design curve. During actual construction, the geological conditions of the tunnel construction area are difficult to predict accurately. To ensure project quality, the working section is often expanded beyond the design surface, and over-excavation construction is generally carried out. The deformation data for each monitoring point align with the actual construction situation on site. This is because, after tunnel construction, the pressure on the top of the tunnel is much greater than the pressure on both sides, causing the entire tunnel to sink noticeably at the top position with no significant change in the horizontal direction, which is a reasonable deformation.

Table 2. Diagnostic analysis results of tunnel excavation deformation.

Monitoring Point	Theoretical Position		S1 Cross-Section Point Cloud Position		S2 Cross-Section Point Cloud Position		Direction Deviation (cm)	
	X (m)	Y (m)	X (m)	Y (m)	X (m)	Y (m)	S1 D _{xy}	S2 D _{xy}
P01	-7.2066	3.2451	-7.2848	3.2123	-7.2916	3.2156	-8.48	-9.00
P02	-6.2435	6.0158	-6.2528	6.1165	-6.2549	6.1198	10.11	10.46
P03	-3.6656	8.7455	-3.5359	8.8864	-3.5366	8.9806	19.15	26.82
P04	0	9.6355	0	9.8339	0	9.9164	19.84	-28.09
P05	3.6301	8.739	3.4960	8.8929	3.484	8.9508	20.41	25.73
P06	6.2188	6.2516	6.2501	6.1369	6.2523	6.1304	-11.89	12.57
P07	7.2142	3.1214	7.2612	3.1618	7.2656	3.1659	6.20	6.80

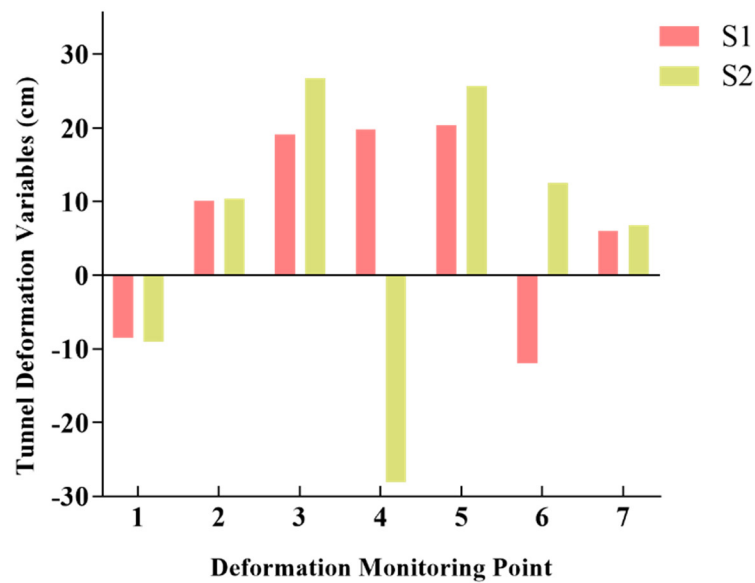


Figure 12. Deformation results of twin in-tunnel excavation.

As an important reference for effectiveness evaluation, the accuracy and efficiency of the algorithm are crucial factors for its potential widespread adoption and application in practical production scenarios. This paper innovatively incorporates a knowledge graph, aiming to enhance the accuracy of deformation detection through knowledge-based guidance. Building on the deformation search threshold calculation for the tunnel excavation scene outlined in Section 2.3 of this paper, the optimal comparison point set is derived through threshold range constraints. Table 3 illustrates the deformation position detection method presented in this paper under the same geometric deformation of the tunnel excavation contour. Compared to conventional methods, the deformation detection accuracy of the proposed method is improved by approximately 47%, significantly enhancing the accuracy of deformation detection and aiding in the efficiency of deformation diagnosis and analysis.

Table 3. Comparison of accuracy of tunnel excavation deformation diagnosis results.

Monitoring Point	Theoretical Position		Control Group			Experimental Group (With Knowledge Constraints)			Accuracy Improvement
	X (m)	Y (m)	X (m)	Y (m)	Direction Deviation	X (m)	Y (m)	Direction Deviation	
P01	-7.2066	3.2451	-7.2848	3.2123	0.0848	-7.2554	3.2310	0.0508	40.10%
P02	-6.2435	6.0158	-6.2528	6.1165	0.1011	-6.2498	6.0903	0.0748	45.75%
P03	-3.6656	8.7455	-3.5359	8.8864	0.1915	-3.5954	8.8229	0.1045	45.44%
P04	0	9.6355	0	9.8339	0.1984	0	9.7410	0.1055	46.82%
P05	3.6301	8.739	3.4960	8.8929	0.2041	3.5677	8.8155	0.0987	51.64%
P06	6.2188	6.2516	6.2501	6.1369	0.1189	6.2408	6.1948	0.0609	48.77%
P07	7.2142	3.1214	7.2612	3.1618	0.0620	7.2447	3.1445	0.0383	48.36%

Table 4 illustrates the difference in total processing time between Cloud Compare and the method described in this paper for detecting geometric deformation of the same tunnel excavation profile. With identical device parameter settings and hardware configurations, the results indicate that the overall computation time of the diagnostic algorithm introduced in this paper is less than 5 min for data volumes on the order of 100,000, whereas the total processing time using Cloud Compare software (2.13.0) exceeds 100 min. In comparison to Cloud Compare, the total time consumption of this method is significantly reduced, enhancing overall efficiency by more than 90%. This paper's method does not

require setting relevant parameters, which lowers the demands on the knowledge and experience of operators and eliminates the need for complex human–computer interaction. It offers considerable advantages in handling complex tunnel twin models. The data processing efficiency in the measurement industry is noticeably superior to Cloud Compare, directly addressing the issue of time-consuming direct comparison methods in large-scale data scenarios.

Table 4. Comparison with Cloud Compare software.

Monitoring Mileage Range	Data Scale (Points)	Time Consumed (min)		Efficiency Improvement
		Cloud Compare Processing	Method of Processing in This Paper	
1 # Tunnel Twin Model	182,359	31.14	2.75	91.17%
2 # Tunnel Twin Model	236,877	32.86	3.12	90.50%
3 # Tunnel Twin Model	240,688	36.18	3.57	90.13%
4 # Tunnel Twin Model	276,445	39.45	4.11	89.58%
5 # Tunnel Twin Model	199,709	30.25	3.08	89.98%

3.2.2. Experiment and Analysis of Visual Cognition

Furthermore, this paper compares and analyzes the cognitive efficiency of visualizing tunnel diagnostic information. It selects diagnostic data from a specific period of tunnel excavation and organizes and displays the content in three distinct ways. First, this paper documents the 3D coordinates and deformation values of each point in tabular form, referred to as the basic group. Second, building on the table data, this paper employs three-dimensional visualization to depict the location of each point and allows for the inspection of each point’s deformation value, termed the display group. Lastly, this paper adopts the visualization method described in Section 2.4 to integrate multiple visual variables, showcasing both the position and deformation value of the points, known as the augmentation group. This approach is depicted in Figure 13.

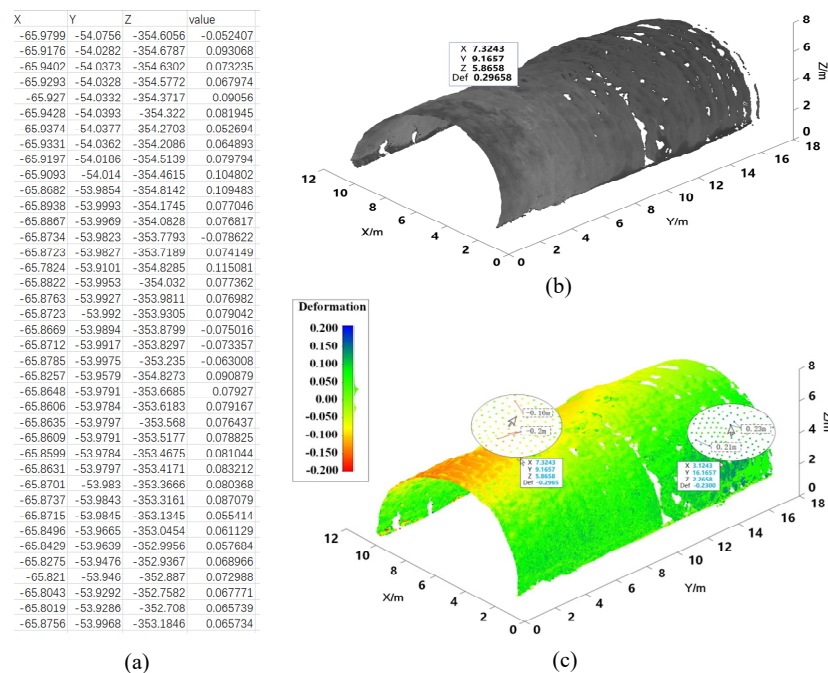


Figure 13. Visualization results of twin deformation in-tunnel excavation. (a) Base group. (b) Display group. (c) Augmentation group.

Each group searched for 20 individuals to conduct experiments, and the experimental process is as follows:

1. Introduce the meaning of the data to participants;
2. Distribute tasks to participants, who need to search for 10 points with a deformation value of -0.16 in the visualization materials of their group;
3. Participants wear an eye tracker to search for points and record the time for each point they find;
4. Wait for the participants to complete the search for 10 points, stop the timer, and end the experiment.

The experimental results are illustrated in Figure 14. As the number of search points increases, the time spent in the base group also increases. For the display group and the enhancement group, due to the clustering effect of space, the increment of time spent on finding other points is relatively stable after finding the first point. For the augmentation group, the speed of finding the initial point was significantly accelerated due to the help of multiple visual variables. The cognitive efficiency of this method is more than 70% higher than that of form viewing and more than 50% higher than that of simple 3D visualization.

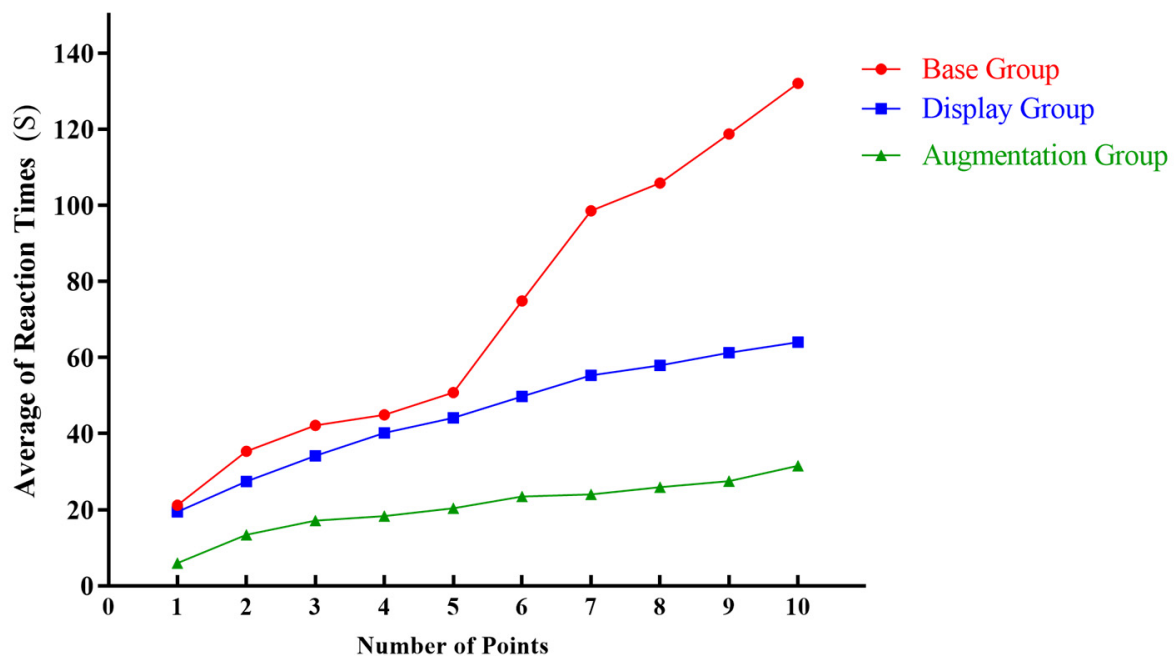


Figure 14. Average reaction times.

Furthermore, the eye movement distribution results were observed, with the findings illustrated in Figure 15. In the basic group, the gaze range of participants is primarily concentrated on the column listing the deformation values, as they search for the corresponding values. Attention shifts to the coordinates of the point only after the correct value is identified. In the display group, the gaze range of participants is quite dispersed, with a global observation pattern. Conversely, in the augmentation group, the focus is more concentrated on areas where the deformation values change, enabling quicker identification of the relevant points.

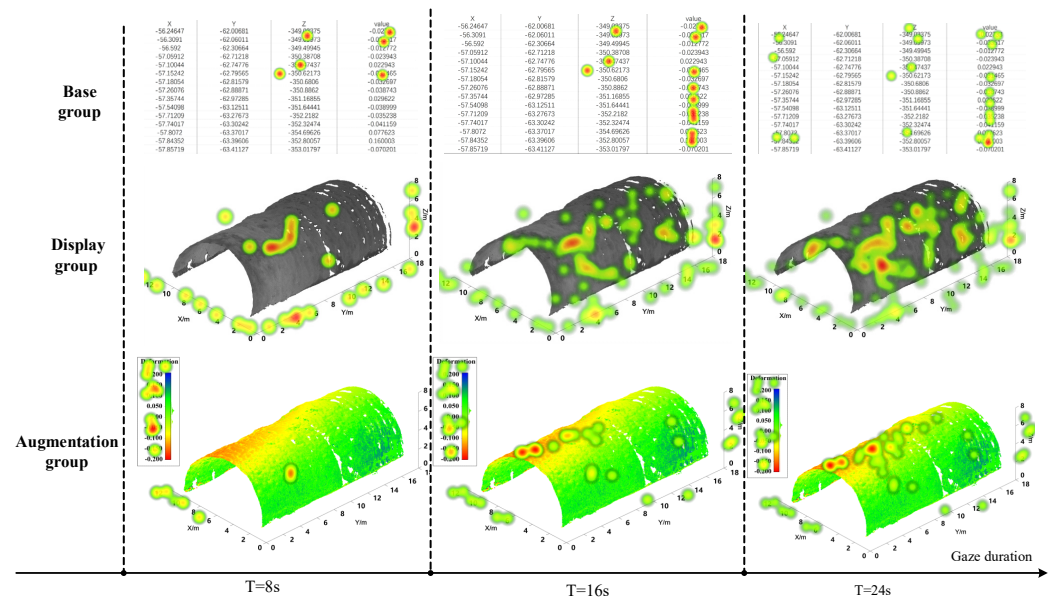


Figure 15. Eye heat distribution results.

4. Conclusions and Future Work

Digital twin scenes can accurately portray the dynamic changes in the geographic environment, effectively promoting tunnel engineering toward intelligent construction [39]; however, lacking a diagnostic analysis function makes it difficult for geographic twin models to reflect the actual engineering situation in the physical world promptly. Therefore, we proposed a knowledge-guided intelligent analysis method of geographic digital twin models, taking the tunnel excavation scenario as an example, and innovatively integrated the knowledge graph technology into diagnosing and visualizing the geometric deformation of the tunnel excavation profile. We improved the automation level of tunnel profile geometry calculation and constructed a tunnel excavation twin scene that meets the public perception. Our method provides a new paradigm for the diagnostic analysis of geographic twin models, which can effectively support the refined management of the tunnel excavation process. Specifically, the practical contributions of this paper are mainly threefold.

First, we constructed a twin scene knowledge graph that considered the dynamic process of tunnel excavation and realized the efficient management of dynamic data of tunnel excavation engineering. On the one hand, the constructed knowledge graph guides the subsequent geometrical deformation diagnosis and visualization expression; on the other hand, it accurately portrays the twin scene objects of the tunnel excavation profile and their interrelationships. It effectively improves the information processing efficiency in tunnel excavation engineering.

Second, we innovatively utilized a knowledge graph to guide the diagnostic process of geometric deformation of the tunnel excavation profile, realizing the rapid diagnosis of the tunnel excavation profile. Through the knowledge graph's guidance, the proposed method's deformation detection accuracy is improved by about 47% compared with the general method, and the diagnosis efficiency is enhanced by more than 90% compared with the commercial software Cloud Compare. In addition, the diagnostic process of the method in this paper does not need to set relevant parameters. It requires less knowledge and experience of the operator, which significantly improves the processing efficiency and automation of tunnel profile geometric deformation calculation.

Finally, we combined multiple visual variables to represent the fusion of tunnel excavation profile diagnostic information and constructed a tunnel excavation twin scene that users can quickly recognize. Eye-movement-based cognitive experiments show that the scene we created can effectively enhance people's understanding of the complex information of tunnel excavation, and the cognitive efficiency is improved by more than 70%

compared to viewing with a form and more than 50% compared to simple 3D visualization. It realizes the efficient expression of the diagnostic and analytical results of the geographic twin model.

However, the method in this paper mainly focuses on the external geometric features of the tunnel and does not consider the structural forces. Therefore, in our future work, we will consider combining finite elements and adding mechanical analysis to deepen the deformation diagnosis of tunnel profile twins. In addition, the participants of the experiments in this paper are all from China and are limited in number. In the future, we will recruit more people from different countries and races to participate in our cognitive experiments to help us further improve the information transfer capability of the tunnel excavation twin scenes to support the intelligent construction of tunnel excavation better.

Author Contributions: Conceptualization, Ce Liang; Writing—original draft, Ce Liang; Data curation, Ce Liang, Jun Zhu, Qing Zhu, Jianlin Wu, Jinbin Zhang, and Jianbo Lai; Methodology, Ce Liang; Software, Ce Liang, Qing Zhu, Jianlin Wu, Jinbin Zhang, Jianbo Lai, and Jingyi Lu; Formal analysis, Ce Liang, Jun Zhu, Jinbin Zhang, Jianlin Wu, and Jingyi Lu; Investigation, Ce Liang, Jun Zhu, Qing Zhu, Jianbo Lai, and Jingyi Lu; Validation, Ce Liang. All authors have read and agreed to the published version of the manuscript.

Funding: This research was funded by the National Natural Science Foundation of China, grant number [42271424] [42171397].

Data Availability Statement: The data that support the findings of this study are available in Available online: <https://figshare.com/s/532e10d8c81aaf720c39> (accessed on 16 December 2023).

Conflicts of Interest: The authors declare that they have no known competing financial interests or personal relationships that could have influenced the work reported in this study.

References

- Huang, W.; Zhang, Y.; Zeng, W. Development and application of digital twin technology for integrated regional energy systems in smart cities. *Sust. Comput.* **2022**, *36*, 100781. [CrossRef]
- Lee, A.; Lee, K.; Kim, K.; Shin, S. A geospatial platform to manage large-scale individual mobility for an urban digital twin platform. *Remote Sens.* **2022**, *14*, 723. [CrossRef]
- Nica, E.; Popescu, G.; Poliak, M.; Kliestik, T.; Sabie, O. Digital Twin Simulation Tools, Spatial Cognition Algorithms, and Multi-Sensor Fusion Technology in Sustainable Urban Governance Networks. *Mathematics* **2023**, *11*, 1981. [CrossRef]
- Yang, J.; Zhang, Y.; Zhu, Z.; Fu, J.; Xie, Z.; Wang, L. Study on tunnel under-over break detection method based on three-dimensional image reconstruction technology. *J. Cent. South Univ.* **2020**, *51*, 714–723.
- Song, S.; Xu, G.; Bao, L.; Xie, Y.; Lu, W.; Liu, H.; Wang, W. Classifying the surrounding rock of tunnel face using machine learning. *Front. Earth Sci.* **2023**, *10*, 2179. [CrossRef]
- Li, J.; Jing, L.; Zheng, X.; Li, P.; Yang, C. Application and outlook of information and intelligence technology for safe and efficient TBM construction. *Tunn. Undergr. Space Technol.* **2019**, *93*, 103097. [CrossRef]
- Tian, S.; Wu, K.; Wang, Z.; Ma, W.; Yi, W. Development Status and Implementation Path Analysis on Intelligent Construction of Mountain Tunnels in China. *J. China Railw. Soc.* **2022**, *44*, 134–142.
- Tao, F.; Liu, W.; Liu, J.; Liu, X.; Liu, Q.; Ting, Q.; Hu, T.; Zhang, Z.; Xiang, F.; Xu, W.; et al. Digital twin and its potential application exploration. *Comput. Integr. Manuf. Syst.* **2018**, *24*, 1–18.
- Opoku, D.; Perera, S.; Osei-Kyei, R.; Rashidi, M. Digital twin application in the construction industry: A literature review. *J. Build. Eng.* **2021**, *40*, 102726. [CrossRef]
- Uhlemann, T.; Schock, C.; Lehmann, C.; Freiburger, S.; Steinhilper, R. The digital twin: Demonstrating the potential of real time data acquisition in production systems. *Procedia Manuf.* **2017**, *9*, 113–120. [CrossRef]
- Wu, Y.; Zhou, Z.; Shao, S.; Zhao, Z.; Hu, K.; Wang, S. Monitoring and Analysis of Deformation Refinement Characteristics of a Loess Tunnel Based on 3D Laser Scanning Technology. *Appl. Sci.* **2022**, *12*, 5136. [CrossRef]
- Ye, J.; Che, D.; Ma, B.; Liu, Q.; Qiu, K.; Shang, X. Construction Method for a Three-Dimensional Tunnel General Monomer Model Based on Parallel Pathfinding. *ISPRS Int. J. Geo-Inf.* **2023**, *12*, 270. [CrossRef]
- Yu, G.; Wang, Y.; Mao, Z.; Hu, M.; Sugumaran, V.; Wang, Y.K. A digital twin-based decision analysis framework for operation and maintenance of tunnels. *Tunn. Undergr. Space Technol.* **2021**, *116*, 104125. [CrossRef]
- Grégorio, J.; Lartigue, C.; Thiébaud, F.; Lebrun, R. A digital twin-based approach for the management of geometrical deviations during assembly processes. *J. Manuf. Syst.* **2021**, *58*, 108–117. [CrossRef]
- Wang, L.; Xu, S.; Qiu, J.; Wang, K.; Ma, E.; Li, C.; Guo, C. Automatic monitoring system in underground engineering construction: Review and prospect. *Adv. Civ. Eng.* **2020**, *2020*, 3697253. [CrossRef]

16. Sabato, A.; Niezrecki, C.; Fortino, G. Wireless MEMS-based accelerometer sensor boards for structural vibration monitoring: A review. *IEEE Sens. J.* **2016**, *17*, 226–235. [[CrossRef](#)]
17. Shiau, J.; Keawsawasvong, S.; Seehavong, S. Stability of Unlined Elliptical Tunnels in Rock Masses. *Rock Mech. Rock Eng.* **2022**, *55*, 7307–7330. [[CrossRef](#)]
18. Li, W.; Zhu, J.; Fu, L.; Zhu, Q.; Xie, Y.; Hu, Y. An augmented representation method of debris flow scenes to improve public perception. *Int. J. Geogr. Inf. Sci.* **2021**, *35*, 1521–1544. [[CrossRef](#)]
19. Jiang, Q.; Zhong, S.; Pan, P.; Shi, Y.; Guo, H.; Yang, J. Observe the temporal evolution of deep tunnel's 3D deformation by 3D laser scanning in the Jinchuan No. 2 Mine. *Tunn. Undergr. Space Technol.* **2020**, *97*, 103237. [[CrossRef](#)]
20. Cui, H.; Ren, X.; Mao, Q.; Hu, Q.; Wang, W. Shield subway tunnel deformation detection based on mobile laser scanning. *Autom. Constr.* **2019**, *106*, 102889. [[CrossRef](#)]
21. Han, J.; Guo, J.; Jiang, Y. Monitoring tunnel profile by means of multi-epoch dispersed 3-D LiDAR point clouds. *Tunn. Undergr. Space Technol.* **2013**, *33*, 186–192. [[CrossRef](#)]
22. Shen, Y.; Wang, J.; Wang, J.; Duan, W.; Ferreira, V. Methodology for extraction of tunnel cross-sections using dense point cloud data. *J. Geodesy Geoinform. Sci.* **2021**, *4*, 56.
23. Zhou, Z.; Zhao, J.; Tan, Z.; Zhou, X. Mechanical responses in the construction process of super-large cross-section tunnel: A case study of Gongbei tunnel. *Tunn. Undergr. Space Technol.* **2021**, *115*, 104044. [[CrossRef](#)]
24. Liu, W.; Chen, J.; Chen, L.; Luo, Y.; Shi, Z.; Wu, Y. Nonlinear deformation behaviors and a new approach for the classification and prediction of large deformation in tunnel construction stage: A case study. *Eur. J. Environ. Civil Eng.* **2022**, *26*, 2008–2036. [[CrossRef](#)]
25. Guo, Y.; Zhu, J.; You, J.; Pirasteh, S.; Li, W.; Wu, J.; Lai, J.; Dang, P. A dynamic visualization based on conceptual graphs to capture the knowledge for disaster education on floods. *Nat. Hazards* **2023**, *119*, 203–220. [[CrossRef](#)]
26. Lai, J.B.; Zhu, J.; Luo, N.Y.; Zhang, Y.; Zuo, L.; Guo, Y.K.; You, J.G. Visual supervision of large-scope heat source factories based on knowledge graph. *Trans. GIS* **2023**, *27*, 408–424. [[CrossRef](#)]
27. Zhu, J.; Luo, N.; Guo, Z.; Lai, J.; Zuo, L.; Zhang, C.; Guo, Y.; Hu, Y. Feature-constrained automatic geometric deformation analysis method of bridge models toward digital twin. *Int. J. Digit. Earth* **2024**, *17*, 2312219. [[CrossRef](#)]
28. Mai, G.; Huang, W.; Cai, L.; Zhu, R.; Lao, N. Narrative cartography with knowledge graphs. *J. Geovisualization Spat. Anal.* **2022**, *6*, 4. [[CrossRef](#)]
29. Zhu, J.; Dang, P.; Cao, Y.; Lai, J.; Guo, Y.; Wang, P.; Li, W. A flood knowledge-constrained large language model interactable with GIS: Enhancing public risk perception of floods. *Int. J. Geogr. Inf. Sci.* **2024**, 1–23. [[CrossRef](#)]
30. Wu, J.; Zhu, J.; Zhang, J.; Dang, P.; Li, W.; Guo, Y.; Fu, L.; Lai, J.; You, J.; Xie, Y.; et al. A dynamic holographic modelling method of digital twin scenes for bridge construction. *Int. J. Digit. Earth* **2023**, *16*, 2404–2425. [[CrossRef](#)]
31. Fu, L.; Zhu, J.; Li, W.; Zhu, Q.; Xu, B.; Xie, Y.; Zhang, Y.; Hu, Y.; Dang, P.; You, J. Tunnel vision optimization method for VR flood scenes based on Gaussian blur. *Int. J. Dig. Earth* **2021**, *14*, 821–835. [[CrossRef](#)]
32. Zhu, J.; Zhang, J.; Zhu, Q.; Li, W.; Wu, J.; Guo, Y. A knowledge-guided visualization framework of disaster scenes for helping the public cognize risk information. *Int. J. Geograph. Inform. Sci.* **2024**, 1–28. [[CrossRef](#)]
33. Mulangi, R.H.; Kulkarni, V. Visualization and assessment of the effect of roadworks on traffic congestion using AVL data of public transit. *J. Geovisualization Spat. Anal.* **2022**, *6*, 28.
34. Li, W.; Zhu, J.; Dang, P.; Wu, J.; Zhang, J.; Fu, L.; Zhu, Q. Immersive virtual reality as a tool to improve bridge teaching communication. *Expert Syst. Appl.* **2023**, *217*, 119502. [[CrossRef](#)]
35. Zhang, J.; Zhu, J.; Dang, P.; Wu, J.; Zhou, Y.; Li, W.; Guo, Y.; You, J. An improved social force model (ISFM)-based crowd evacuation simulation method in virtual reality with a subway fire as a case study. *Int. J. Digit. Earth* **2023**, *16*, 1186–1204. [[CrossRef](#)]
36. Dang, P.; Zhu, J.; Zhou, X.; Rao, Y.; You, J.; Wu, J.; Zhang, M.; Li, W. A 3D-Panoramic fusion flood enhanced visualization method for VR. *Environ. Model. Softw.* **2023**, *169*, 105810. [[CrossRef](#)]
37. Li, W.; Zhu, J.; Zhu, Q.; Zhang, J.; Han, X.; Dehbi, Y. Visual attention-guided augmented representation of geographic scenes: A case of bridge stress visualization. *Int. J. Geograph. Inform. Sci.* **2024**, *38*, 527–549. [[CrossRef](#)]
38. Ying, S.; Van Oosterom, P.; Fan, H. New Techniques and Methods for Modelling, Visualization, and Analysis of a 3D City. *J. Geovisualization Spat. Anal.* **2023**, *7*, 26. [[CrossRef](#)]
39. Li, W.; Zhu, J.; Fu, L.; Zhu, Q.; Gong, Y. A rapid 3D reproduction system of dam-break floods constrained by post-disaster information. *Environ. Modell. Softw.* **2021**, *139*, 104994. [[CrossRef](#)]

Disclaimer/Publisher's Note: The statements, opinions and data contained in all publications are solely those of the individual author(s) and contributor(s) and not of MDPI and/or the editor(s). MDPI and/or the editor(s) disclaim responsibility for any injury to people or property resulting from any ideas, methods, instructions or products referred to in the content.